Synthesis and Characterization of Double Perovskite, La_2NiMnO_6 by Solid State Method

A

Project Report

Submitted in partial fulfillment of the requirement for the award

Of the degree of

MASTER OF TECHNOLOGY

In

NANOSCIENCE AND TECHNOLOGY

By

SACHIN DUA

Roll no. 2K14/NST/10

Under the Guidance of

Dr. Amrish K.Panwar

Assistant Professor

DEPARTMENTNT OF APPLIED PHYSICS

DELHI TECHNOLOGY UNIVERSITY

NEW DELHI – 110042

JUNE - 2016

Department of Applied Physics

Delhi Technological University

Delhi

CERTIFICATE

This is to certify that Mr. Sachin Dua, a student of final semester M. Tech. (Nanoscience and Technology), Applied Physics Department, during the session 2014-2016 has successfully completed the project work on **"Synthesis and Characterization of Double Perovskite, La_2NiMnO_6 by Solid State Method"** at DTU, Delhi and has submitted a satisfactory report in partial fulfillment for the award of the degree of Master of Technology.

The assistance and help received during the course of investigation have been fully acknowledged. He is a good student and we wish him good luck in future.

Dr. Amrish K. Panwar
Assistant Professor,
Applied Physics Department
Delhi Technological University
Delhi - 110042

Prof. S.C. Sharma
HOD
Applied Physics Department
Delhi Technological University,
Delhi - 110042

Candidate Declaration

I hereby declare that the work which is being presented in this thesis entitled **"Synthesis and Characterization of Double Perovskite, La_2NiMnO_6 by Solid State Method"** is my own work carried out under the guidance of Dr. Amrish K. Panwar, Assistant Professor, Delhi Technological University, and Delhi.

I further declare that the matter embodied in this thesis has not been submitted for the award of any other degree or diploma.

Date: Sachin Dua

Place: New Delhi Roll No.- 2K14/NST/10

Acknowledgements

With great pleasure I would like to express my first and sincere gratitude to my supervisor **Dr. Amrish K. Panwar** for his continuous support, patience, motivating ideas, enthusiasm and immense knowledge. His guidance always enlightens and helped me to shape my work.

Besides my Supervisor, I would like to express my deep gratitude and respect to **Prof. S.C. Sharma**, Prof. and Head of Department of Physics, DTU, for his encouragement, insightful comments and valuable suggestions during the course.

My sincere thanks also go to **Dr. Pawan Tyagi, Dr. M. Jayasimhadri, Dr. Mohan S. Mehata, Dr. Ajeet Kumar and Dr. Nitin K. Puri** for their valuable advices and stimulating discussions throughout my course work. Thanks them for questioning me about my ideas, helping me think rationally.

I also wish to express my thanks to research scholar Mr. Aditya Jain and Mr. Rakesh Saroha for their cooperation and suggestions during this project. My hearty thanks to all my classmates as well as staff at Department of Applied Physics of Delhi Technological University for their goodwill and support that helped me a lot in successful completion of this project.

Sachin Dua
M. Tech. NST
2K14/NST/19

ABSTRACT

Perovskites exhibit several interesting chemical and physical properties. They can have electronic structures ranging from insulating to metallic and even half metallic with spin-polarized electrical conductivity. They have magnetic orderings ranging from antiferromagnetic to ferri- and ferromagnetic. One such interesting double perovskite which show Multiferroic property is La_2NiMnO_6.

In this work, double perovskite La_2NiMnO_6 samples are prepared by solid state method by three stage thermal treatment. X-ray diffraction confirms the phase purity of La_2NiMnO_6 as well as the crystal structure. The samples are crystallized in monoclinic structure with space group $P2_{1/}n$. The composition, morphology and structural identity of the sample have been characterized by Scanning Electron Microscope (SEM), X-ray Diffraction (XRD) and Energy-Dispersive X-ray spectroscopy (EDX). Temperature dependent dielectric measurement of the sample in the frequency range 1 kHz to 1 MHz shows step like decrease in dielectric constant at lower temperature, and loss tangent show corresponding relaxation peak. Activation energy of the sample is calculated to understand the potential barrier for a reaction.

Contents

List of Figures

List of Tables

CHAPTER 1

Introduction

1.1 Transition Metal Oxides

Transition metal oxides are compounds composed of oxygen atoms combined with transition metal. Transition metals are defined as elements which have partially filled d sub-shell or which can form cations with an incomplete d sub-shell. Due to partially filled d shell, these elements exhibit two or more oxidation states. For example, compounds of Manganese are known in oxidation states between +2, such as MnO and +7, such as Mn_2O_7 [1]. These oxides have various surface structures which influence their chemical properties and affect the surface energy of the compound. The coordination of metal cation and oxygen anion affect the relative acidity and basicity of atoms present on the surface of metal oxides.

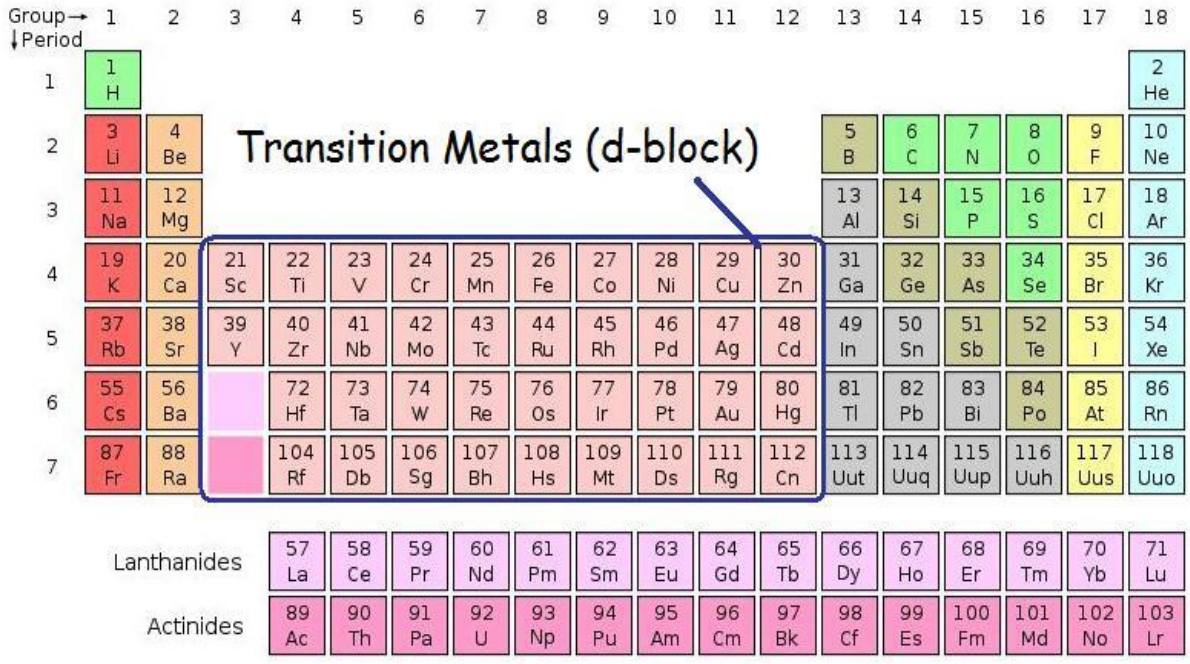

Fig 1.1 Periodic table representing Transition Metals [2]

1.2 Types of Transition Metal Oxides

Transition Metals have wide range of oxidation states and most of these elements have more than one oxidation state. There are various types of transition metal oxides depending on the oxidation states of the element. The crystal structure of these oxides is based on close pack array of oxygen anions with metal cations occupying interstitial sites. The transition metal oxides types are

Monoxides

Transition metals which have oxidation state of +2 form the monoxides. Many transition metal such as TiO, NiO, etc form the monoxides have rocksalt structure. The rocksalt structure is formed by filling all octahedral sites with cations in an oxygen anion fcc array.

Dioxides

Transition metal dioxides have oxidation state of +4 and majority of these oxides have rutile structure such as MnO_2. The rutile structure is generated by filling half of octahedral sites with cations of the hcp oxygen anion array.

Trioxides

Transition metal oxides which have oxidation state of +6 form the trioxides MO_3. Few transition metals such as tungsten (W) can from the trioxides such as WO_3.

Ternary oxides

Ternary oxide contain two elements attach with oxygen such as SrV_2O_6, $Sr_2V_2O_5$, $SrVO_3$. Ternary oxide stoichiometry varies by changing proportion of two compounds and their oxidation states. Combination of two or more compound in an oxide creates lots of structural properties. Prediction of the structures is difficult for ternary oxides. The examples of ternary oxides are perovskite (ABX_3 or $CaTiO_3$). [3]

1.3 Perovskite

Perovskites, named after Russian mineralogist L. A. Perovski, are compound with crystal structure same as that of calcium titanium oxide ($CaTiO_3$) or ABX_3, where 'A' and 'B' are two different sizes cations and X is an anion that bonds to both. Perovskite oxides have intensely being studied over last few decades as they show variety of electrical, magnetic and optical properties. The diverse physical properties shown by perovskites are listed in Table 1.1.

Typical Property	Typical Compounds
Ferroelectric Property	$BaTiO_3$, $PbTiO_3$
Piezoelectricity	$Pb(ZrTi)O_3$, $(BiNa)TiO_3$
Electrical conductivity	ReO_3, $SrFeO_3$, $LaCoO_3$, $LaNiO_3$, $LaCrO_3$
Superconductivity	$La_{0.9}Sr_{0.1}CuO_3$, $YBa_2Cu_3O_7$
Ion conductivity	$La(Ca)AlO_3$, $CaTiO_3$, $BaZrO_3$, $SrZrO_3$, $BaCeO_3$
Magnetic property	$LaMnO_3$, $LaFeO_3$
Catalytic property	$LaCoO_3$, $LaMnO_3$, $BaCuO_3$
Electrode	$La_{0.6}Sr_{0.4}CoO_3$, $La_{0.8}Ca_{0.2}MnO_3$

Table 1.1: Typical properties of Perovskite [4]

1.3.1 Perovskite structure

Perovskite compound with general formula ABO_3 have cubic structure, where A is usually an alkaline earth or rare earth cation (Ca, La, Sr, etc) on the corner of lattice and B could be 3d, 4d, 5d transition metal(Mn, Ni, Fe, etc). The ideal cubic-symmetry structure has A cation in 12 fold cuboctahedron coordination and B cation in 6 fold coordination with oxygen atoms forming BO_6 octahedral. In the cubic unit cell of perovskite compound, type 'A' atom sits at cube corner positions (0, 0, 0), type 'B' atom sits at body center position (1/2, 1/2, 1/2) and oxygen atoms sit at face centered positions (1/2, 1/2, 0).[5] The structure and physical properties are largely depends on nature of B-site cation and the B–O bond lengths of BO_6 octahedral.

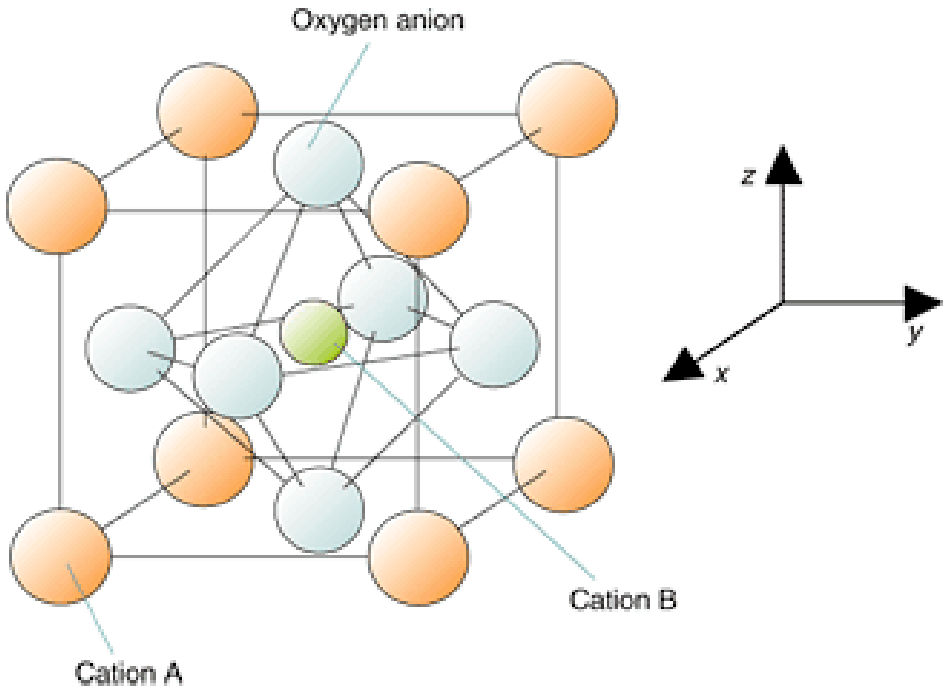

Fig 1.2: Cubic perovskite unit cell [6]

1.4 Double Perovskite

Double perovskite belong to a large family of oxide with general formula $A_2BB'O_6$, where 'A' is an divalent or trivalent alkaline earth ion, B and B' being transition metal ions. The double perovskite structure unit cell is twice that of perovskite i.e. ABO_3.A $B'O_3$. It has the same architecture of 12 coordinate A sites and 6 coordinate B sites, but two cations are ordered on the B site. The B- site cation, B and B' may remain ordered or they can be disordered in the crystal structure. Large number of possible B and B' combinations in double perovskites led to variety of magnetic phases i.e. ferromagnetic, anti-ferromagnetic, spin glass, etc. Partial cation substitution is common method for changing the properties of perovskite compounds. Physical properties of double perovskite depend upon chemical combination of B and B', ionic radius and valency of A-cation.

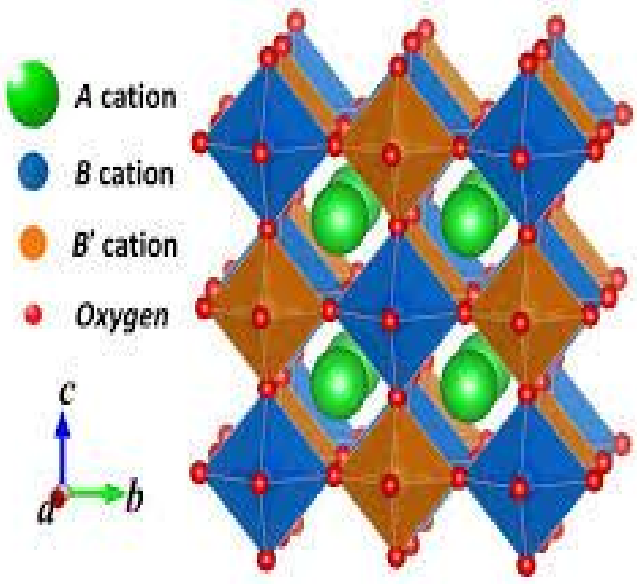

Fig 1.3 Double Perovskite unit cell [7]

1.4.1 Double Perovskite structure

The double perovskite unit cells is twice that of perovskite i.e. overlapping of two perovskite unit cell, therefore it's general formula is $A_2B'B''O_6$, which is $AB'O_3.AB''O_3$. The structure and space group of the $A_2B'B''O_6$ perovskites depends on the B-site cation ordering. The two different cations, B' and B", may remain disordered at the B site, or they can be orderly arrange. The B-site cation can be order in three different ways. The most common case, cations alternate in all three dimensions forming rock-salt like formation which is known as elpasolite structure. The second is rare case of columnar order may take place in which two different B cations alternate in two different directions. The third one in which cation may form layered order i.e. alternate only in one direction, this scenario occur occasionally. The most common type of B-site ordering is the rock-salt order, followed by smaller number of disordered compounds. [8]

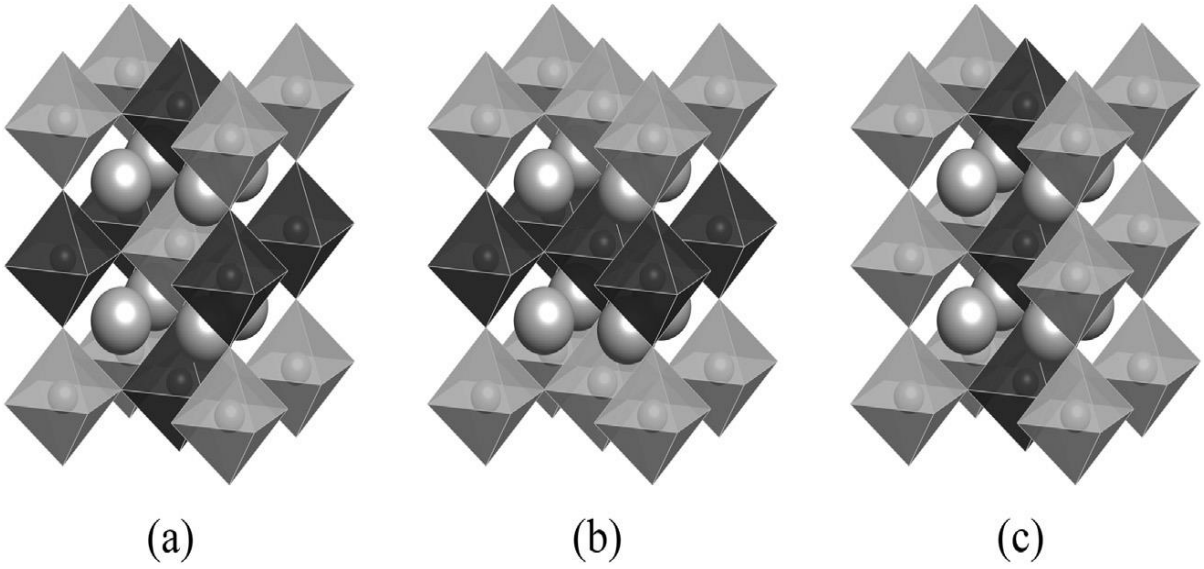

Fig 1.4 Different B-site cation orderings found in $A_2B'B''O_6$ perovskites: (a) rock-salt, (b) layered and (c) columnar order [8]

1.5 La_2NiMnO_6 (LNMO)

It is a double perovskite material. Double perovskite La_2NiMnO_6 ceramics and thin films have been receiving huge scientific interest due to its unique dielectric, magnetic, magnetodielectic characteristics and subsequent potential application such as spin filtering tunnel junction, magnetodielectric capacitors. In this study, we discuss about the surface morphology, composition, phase structure and dielectric properties of the La_2NiMnO_6 ceramics. The surface morphology of the LNMO sample along with its structure, composition and the temperature dependence dielectric properties at various frequencies has been studied. Dielectric constant and loss tangent were also observed at different frequencies by changing the temperature.

CHAPTER 2

Literature Review

2.1 Introduction

There is a recent upsurge of interest in double perovskite since last few decades, compound La_2NiMnO_6 (LNMO), because of its various properties, especially large dielectric anomaly and related potential applications has been studied. Various studies had been conducted to have better understanding of coupling between the phononic, magnetic and electronic degrees of freedom (DOF) because an intricate interplay between these DOF is believed to be responsible for various physical phenomena observed in the material. Ferromagnetic behavior of LNMO at near room temperature has been determined by magnetization and neutron diffraction studies. In the partially disordered single phase monoclinic system multiglass behavior and MC effect have been observed over wide range of temperature due to asymmetric hopping of electrons between Ni^{2+} and Mn^{4+} ions.[9] Magnetodielectric effect shown by the material is due to strong coupling between magnetic and dielectric properties, where the dielectric properties can be controlled by magnetic field. At temperature as high as 280 k large magnetic-field-induced changes occur in the resistivity and dielectric properties of LNMO, which is much higher than the previously observed temperature for such coupling between electric, dielectric and magnetic properties in a ferromagnetic semiconductor. The electric charge, spin, and dielectric properties of LNMO can be tuned by magnetic and /or electric field, which show LNMO is rare example of single material platform with multiple functions.[10] To tune the properties of LNMO various modification has been conducted, such as by substitution of Sr in place of La in LNMO results in transition from ferromagnetic insulating phase to half metallic phase and by increasing the Ti content in $La_2NiMn_{1-x}Ti_xO_6$ transform the material from ferromagnetic phase to antiferromagnetic. Due to dilution effect the dielectric constant monotonically decreases and relaxor-like behavior is suppressed. The dielectric properties of LNMO exhibit sensitively dependence on the synthesis method, sintering condition and electrode.[11] Magnetoresistance (MR) effect, the magnetic field dependent variation in the resistance of the materials, has been studied due to its rich physics and technological application. This phenomenon has been observed in many magnetic oxides, such as the manganites show colossal magnetoresistance (CMR) and the granular perovskite observe tunnelling magnetoresistance (TMR). The TMR effect is caused by the spin-dependent tunnelling between the ferromagnetic (FM) grains and has a better low-field response compared to the intrinsic CMR effect. MR effect had been observed in the LNMO near room-temperature and the magnetic field dependent MR can be divided into two parts of

the low-field MR and the high-field MR. By observing the magnetic and electric properties, it is suggested that the low-field MR can be attributed to the tunnelling effect between the neighbouring FM domains and the high-field MR is caused by the suppression of the scattering from the spin defects caused by the Ni/Mn anti-site disorders. [12] The partially disordered La_2NiMnO_6 has various interesting properties such as disordered ferromagnetism at higher temperatures and a reentrant spin- glass transition at lower temperatures, a relaxor–type dielectric behavior which define this system as rare example of an intrinsic multiglass system. The disorder in the form of antisite defects between Ni and Mn ions played essential role in interrelating these diverse properties. [13] Both La_2NiMnO_6 ceramics and thin films have been studied extensively because of their interesting magnetodielectric characteristics and subsequent potential applications in spintronic devices such as magnetodielectric capacitors and spin filtering tunnel junctions.

2.2 La_2NiMnO_6 Structure

LNMO is polymorphic with two different structures. LNMO show monoclinic or rhombohedral structure based upon temperature which affects the order of the B-site cations. It has monoclinic ($P2_{1/n}$) or orthorhombic (*Pbnm*, with *c* being the long axis) structure at ambient temperature and a rhombohedral (R-3) structure at high temperature. Often, these two phases i.e. monoclinic and orthorhombic coexist at room temperature with majority phase being monoclinic. Neutron diffraction studies indicate a reduction from the orthorhombic symmetry to the monoclinic subgroup $P2_1/n$ due to the *B* cation ordering. Oxygen anion plays important role in dictating structure and physical properties of material, because being at center of the B-O-B bond its presence or absence can greatly influence the valence states, local lattice distortions, as well as the orbital order.[14] One can obtain pure monoclinic phase under stringent synthesis conditions which would determines the formation of monoclinic phases and control the anti-site disorder and the formation of lanthanum and oxygen vacancies. [9] The ferromagnetic LNMO crystallizes in ordered double perovskite structure, in which NiO_6 and MnO_6 are arranged in rock-salt configuration. This ordered Ni^{2+}--O—Mn^{4+} superexchange interactions give rise to high ferromagnetic curie temperature of 280 k.[15] According to the Kanamori–Goodenough (KG) rules, superexchange interaction between Mn^{4+} and Ni^{2+} leads to ferromagnetic (FM), and Ni^{2+}–O^{2-}–Ni^{2+}, Mn^{4+}–O^{2-}–Mn^{4+} are antiferromagnetic (AFM). The appearance of AFM interactions in the FM background would reduce the strength of FM interactions, causing multiple magnetic transitions subsequently.[16]

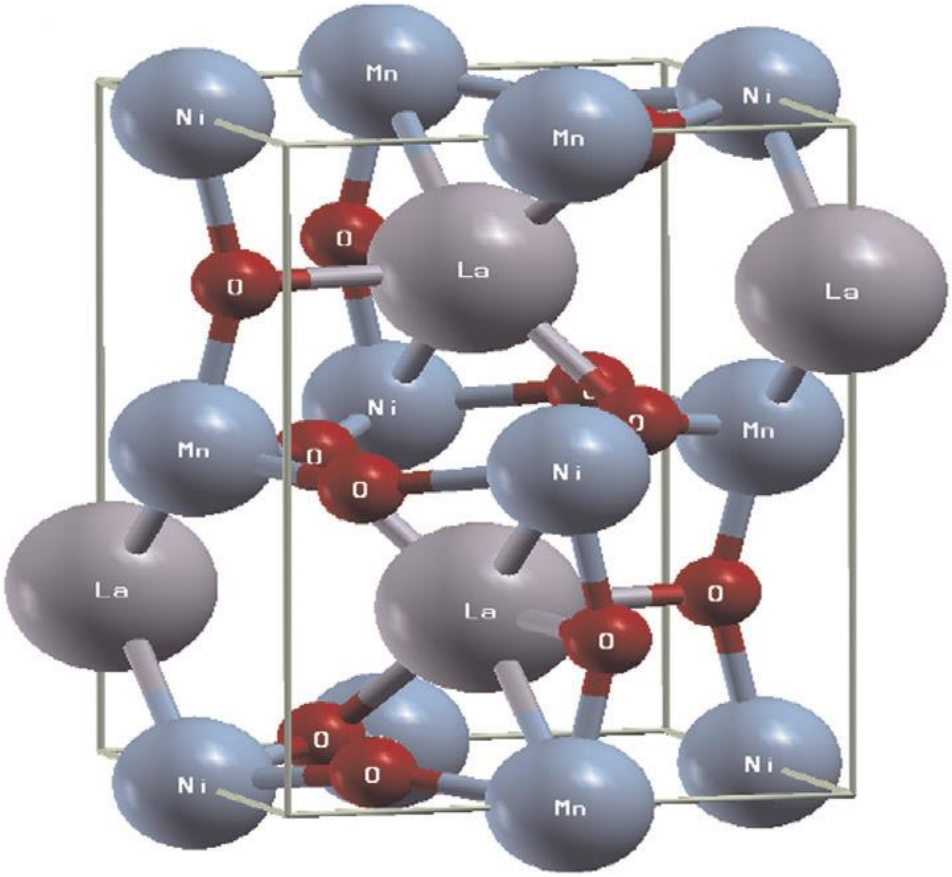

Fig 2.1 Rock-salt structure of unit cell of La_2NiMnO_6 [17]

2.3 Synthesis Techniques

The double perovskite La_2NiMnO_6 can be prepared using solid state method and various wet chemical method. In this we discuss the general wet chemical method which is sol-gel technique. The crystalline structure of the LNMO depends upon the synthesis method and the conditions under which it's synthesis.

2.3.1 Synthesis using sol-gel technique

High purity La_2O_3, $MnCO_3$ and $Ni(NO_3)_2.6H_2O$ compounds were used as the starting ingredients. 5% PVA solution which act as binder for pellets was made by dissolving PVA in deionized water at 80°C. Stoichiometric mixture of La_2O_3 and $MnCO_3$ powders were dissolved in nitric acid and mixed with the PVA solution. Finally, stoichiometric ratio of $Ni(NO_3)_2.6H_2O$ was added to the solution. With continuous heating at 80°C under constant

stirring to evaporate superfluous water, the volume of the solution decreased and the solution viscosity increased continuously. A colloid was formed with the evolution of NOx gas resulting from decomposition of the nitrate ions. Throughout the process, no precipitation was observed. Then, the sample was heated in an oven at 250°C for 2 h. The colloid swelled and self-ignited with a large volume of gases. The auto-ignition resulted in a voluminous La_2NiMnO_6 precursor powder. The prepared powder was calcined at 400–800°C for 2 h in air. [18]

2.3.2 Synthesis using solid state method

La_2NiMnO_6 ceramic was prepared by traditional ceramic processing. By grinding the stoichiometric ratio La_2O_3 (99.99%), NiO (99%), MnO_2 (97.5%) powders with ethanol and then calcined at1473K in air for 7h in alumina crucibles the LNMO powder was synthesized. The calcined powders with 5% polyvinyl alcohol (PVA) were pressed into hydraulic press with the pressure of 98 kPa. Finally, dense LNMO ceramics were sintered at 1773K in air for 4h. The sintered pellets were polished to 1.25mm in thickness. The phase of the specimen was examined by powder X-ray diffraction (XRD) analysis with CuKα radiation. [11]

2.4 Literature survey

La_2NiMnO_6 have received good attention in recent times, because of the ferromagnetic semiconducting behavior and structural stability at high temperatures. Various studies have been conducted to study the structure, dielectric, electrical and magnetic properties of the material and various factors which affects these properties. A few experimental reports of the compound are available in literature. Some of the reference studies have been used for this project. Lin et al. [15] studied the La_2NiMnO_6 ceramic that is crystallized in the monoclinic $P2_{1/n}$ structure in which the Ni^{2+} and Mn^{4+} ions are ordered periodically and the unique relaxor-like dielectric activities along with an enormous dielectric constant step shown by La_2NiMnO_6 (LNMO). Kumar et al. [9] observed that the biphasic LNMO around 270K exhibited the dielectric anomaly where in a single phase LNMO such effect was not seen. Rogado et al. [10] observe the magnetocapacitance and magnetoresistance shown by the LNMO material near room temperature. Cao et al. [11] investigate the influences of electrode material, DC bias and temperature on the electrical and dielectric properties of LNMO

ceramic which revealed the low intrinsic dielectric constant and giant dielectric constant from extrinsic contribution from interface polarization. Choudhury et al. [13] establish that the pure monoclinic bulk phase of partially disordered LNMO compound is an intrinsically multiglass system with a large magnetodielectric coupling (8%–20%) over a wide range of temperatures. Yuan et al. [16] observed the dynamic magnetic behavior of single-phase polycrystalline LNMO material which shows ferromagnetic behavior with Tc about 270K. and superparamagnetic (SPM) behavior at low temperature with frequency dependence. Ullah et al. [17] studied the various electronic, thermoelectric and magnetic properties of La_2NiMnO_6. Li et al. [18] studied the electric field dependence of dielectric constant of the single phase LNMO ceramics using the ‘‘multi-polarization mechanism’’ model.

CHAPTER 3

Synthesis and Characterization of La_2NiMnO_6

3.1 Synthesis Procedure of La_2NiMnO_6 by solid state method

Solid state method is one of the well-known techniques used for the preparation of the sample. The solids can't react with one another at room temperature over limited time period so it's required to heat the solid to much higher temperature in order to attain reaction at satisfactory rate.

The compounds Lanthanum oxide [La_2O_3](99.9%), Nickel oxide [NiO](99.999) and Manganese dioxide [MnO_2](99.99) of Sigma Aldrich were used for the synthesis of La_2NiMnO_6. In the first step all these materials were mixed thoroughly in stoichiometric ratio as 5.349 gm of La_2O_3, 1.225 gm of NiO and 1.426 gm of MnO_2 with the help of mortar and pestle. The grinding of the material was carried for 6-7 hours with acetone as liquid medium for proper mixing. After grinding three stages thermal treatment was attempted. The prepared precursor was calcined in air at 1000°C for 20 hrs followed by slow cooling in ambient temperature. The obtain powder was again sintered in air at 1200°C for 20 hrs. After sintering the powder was pressed into pellets using a hydraulic press. These pellets were sintered in air at 1300°C for 20 hrs to obtain the La_2NiMnO_6 double perovskite. The block diagram of the solid state method is shown in figure 3.1

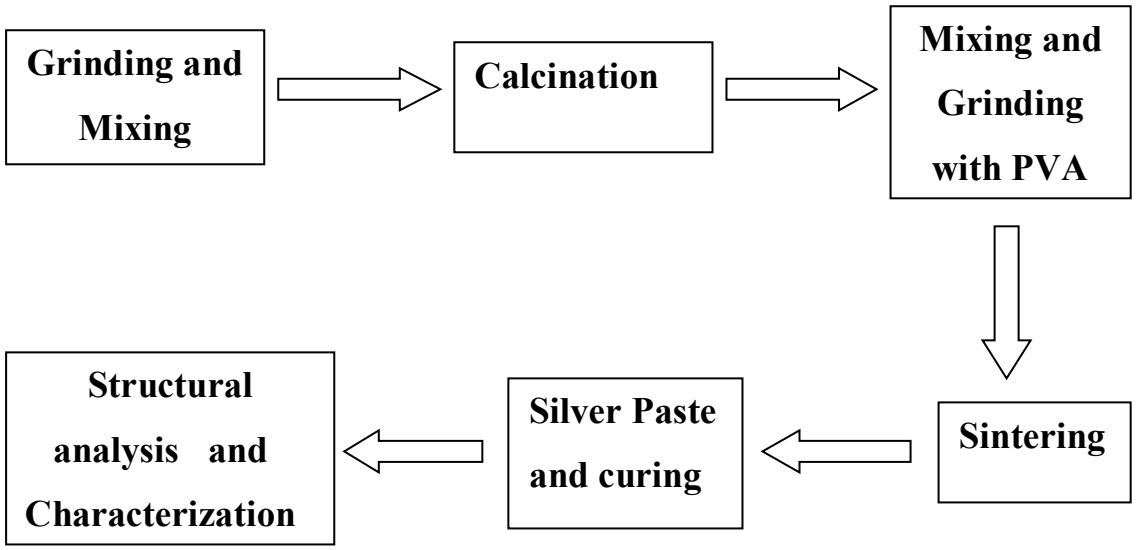

Fig 3.1 Block Diagram representation of solid state method

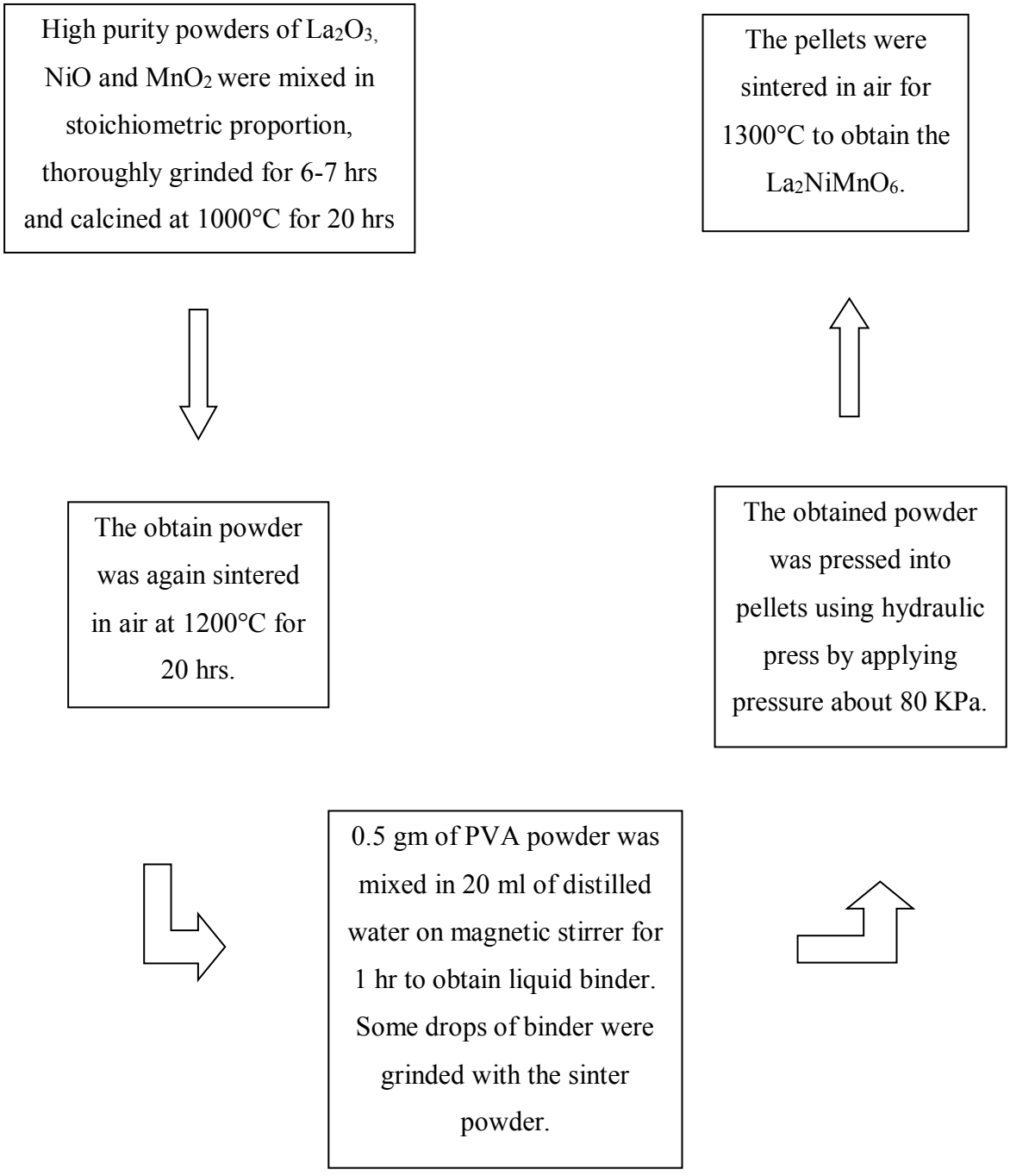

Fig 3.2 Block Diagram for synthesis of La_2NiMnO_6 by solid state method

3.2 **Pellet Formation**

The calcined powder of La_2NiMnO_6 obtained from the solid state method was mixed with PVA binder to form the pellets. 0.5 gm of PVA (poly vinyl alcohol) powder in 20 ml of distilled water was mixed and then stirred for 1 hour to obtain a thick sticky liquid of binder. Few drops of this solution were added to the La_2NiMnO_6 powder and grinded in pestle and mortar for some time. This mixture was pressed into pellets using hydraulic pressing machine by applying pressure about 80 KPa. The pellets were heated at 120°C for 2 hours. These pellets were then coated with silver paste and again heated at 150°C for 2 hours in hot air oven to remove the moisture.

3.3 **Methods of Characterization**

Characterization techniques are the methods from which prepared sample can be easily identify with respect to its composition, surface topology, internal structure, morphology, etc.

These techniques are used to study the properties of the prepared sample. Following techniques were adopted for the characterization.

3.3.1 **X-ray Diffraction (XRD)**

X-ray diffraction technique has been used to get information about crystal structure, crystal composition, lattice parameter, spacing between two crystal planes. X-ray diffraction is based on constructive interference of monochromatic X-rays and a crystalline sample and is determine by Bragg's law. When X-ray collides with the sample particles, X-ray are diffracted according to the electron and x-ray collision. The structure of the sample and wavelength effects the X-ray diffraction pattern.

X-rays are the waves of electromagnetic radiation and crystals are array of atoms in which atoms are periodically arranged. When X-ray waves collide with periodic atoms then waves are scattered in backward direction. X-ray striking an electron would produces secondary spherical waves emanating from the electron. This phenomenon is called as elastic scattering and the electron is called scatterer. A regular array of spherical waves is produces by the regular array of scatterers. Most of these waves cancel one another through destructive interference, however, in few specific directions they add constructively. This constructive interference of forward and backward waves is responsible for obtaining the information about XRD which can be determine by Bragg's law.

According to the Bragg law,

$$2d\sin\theta = n\lambda$$

Where θ is scattering angle, d is the spacing between diffracting planes, n is any integer, and λ is the wavelength of the X-ray beam.

X-rays wavelength λ generally have the same order of magnitude as the spacing d between planes in the crystal therefore, X-rays are used to produce the diffraction pattern.

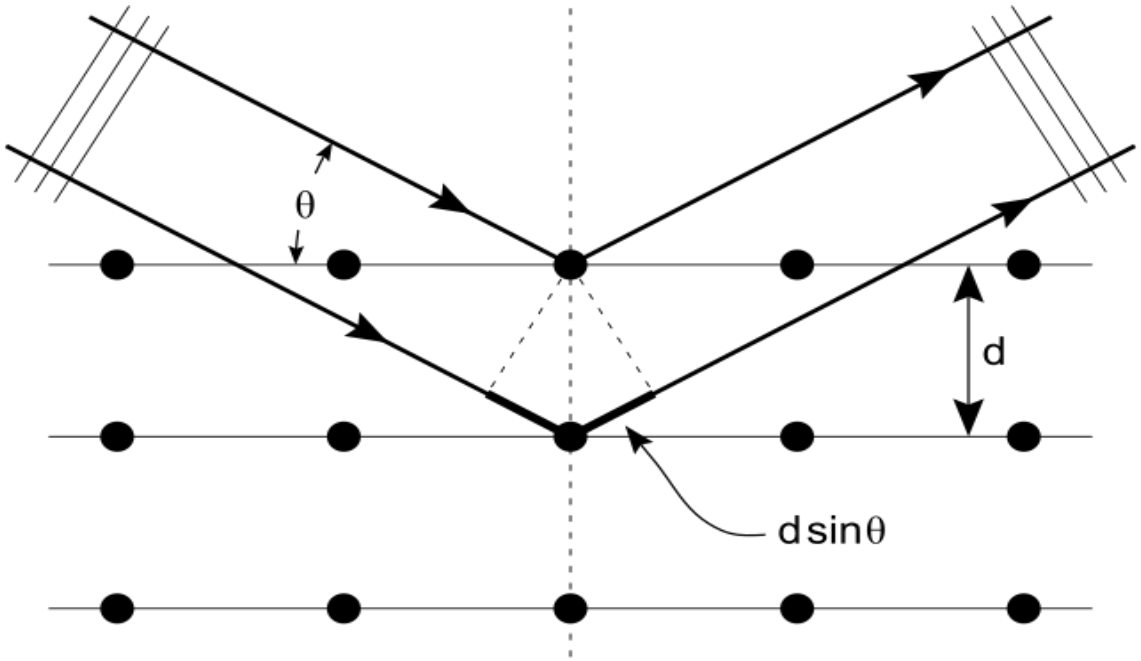

Fig 3.3 Bragg's diffraction [19]

As shown in fig 3.3, the incoming beam causes each electron to re-radiate a small portion of its intensity as spherical wave. If these electrons are arranged in symmetrically with separation d, then the spherical waves will be in sync or there would be constructive interference only in directions where there path length difference 2dsinθ equals an integer multiple of the wavelength λ.

X-ray diffractometers consist of three basic elements: an X-ray tube, a sample holder, and an X-ray detector. X-rays are generated in cathode ray tube by heating a filament to produce electrons. These electrons are accelerated by applying voltage and bombarded on the target material when have sufficient energy to dislodge inner shell electrons of the target material, characteristic X-ray spectra are produced. These X-rays have different wavelength for specific material. The continuous rotation of sample and detector is done and intensity is recorded. When the geometry of incident X-ray satisfies Bragg's equation, constructive interference take place and intensity is observed in the form of peaks. A detector records and processes this X-ray signal and converts the signal to a count rate which is then output to a device. The geometry of an X-ray diffractometer is such that the sample rotates in the path of the collimated X-ray beam at an angle θ while the X-ray detector is mounted on an arm to collect the diffracted X-rays and rotates at an angle of 2θ.

Fig 3.4 X-ray diffraction equipment used in the XRD characterization of La_2NiMnO_6

3.3.2 **Scanning Electron Microscope (SEM)**

A scanning electron microscope (SEM) is a type of electron microscope which produces images of a sample by scanning it with the help of focused beam of electrons. When the electrons interact with sample's atom, it produces various signals which contain information about surface topography, crystallography, morphology and composition of the sample. Raster scan pattern is generally used by electron beam to scan the sample. The beam position is combined with detected signal to create an image. The various signal produce by SEM include secondary electrons, back-scattered electrons, transmitted electrons, light (cathodoluminescence) and photons of characteristic X-rays. However, Secondary electron detectors are standard in all SEMs and most don't have detectors for all the signals. The angle on which incident beam contacts the surface of sample affect the detected number of secondary electrons. Using special detector for scanning the surface and collecting secondary electrons which are emitted an image displaying the topography of surface can be created.

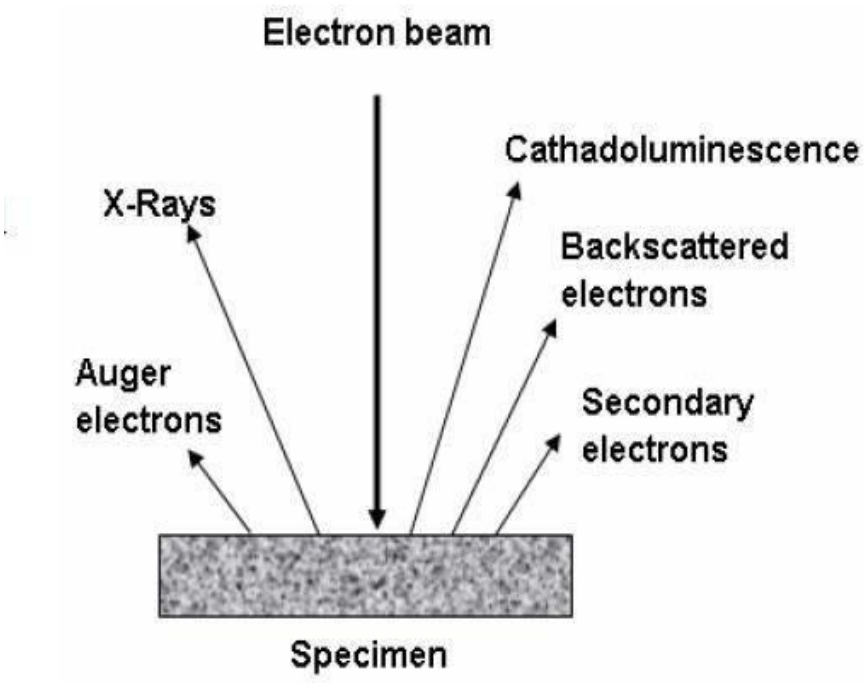

Fig 3.5 Different types of electron released during SEM imaging [20]

An electron beam of SEM is emitted from an electron gun which is equipped with the tungsten filament cathode. The electron beam generally have energy of the order ranging from 0.2 to 40 keV, this beam is pointed by one or two condenser lenses for a spot having the diameter 0.4 nm to 5 nm. Then the beam is passed through pairs of deflector plate or couple of scanning coils existing in electron column, and lastly through deflector lens, that deflects the beam and scan in a raster way to cover a rectangular area in x and y axes of the sample's surface. The scanning process starts from top to bottom and from left to right. The raster pattern is used to produce the image on monitor screen.

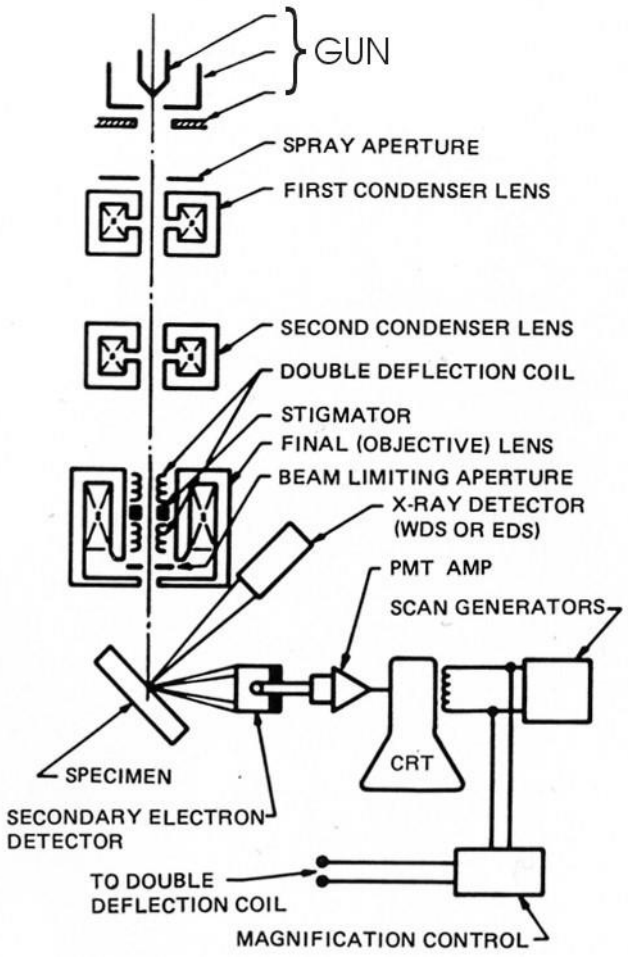

Fig 3.6 Schematic drawing of the electron and x-ray optics of SEM-EPMA [21]

Fig 3.7 Scanning electron microscope equipment used in the SEM characterization of La_2NiMnO_6

3.3.3 Energy Dispersive Spectroscopy (EDS)

It is also known as energy dispersive X-ray analysis (EDXA) or energy dispersive X-ray microanalysis (EDXMA). This analytic technique is used for chemical characterization or elemental analysis of a sample. It works on the principle that all elements of periodic table have different atomic structure and thus they have different set of peaks in x-ray spectrum. To stimulate the emission of characteristic X-rays from the sample, a high-energy beam of charged particles is focused into the sample. EDS may be equipped with SEM and help in identify the elements in any sample. The main disadvantage of EDS is that it does not show significant peaks for element having molecular weight less than 11, i.e. $Z<11$.

3.3.4 **Dielectric Spectroscopy**

It is also known as impedance spectroscopy or electrochemical impedance spectroscopy (EIS). . Dielectric and impedance spectroscopy measures electrical properties of material as it is subjected to periodic electric field to characterize its molecular kinetics. It measures the dielectric properties of a material as a function of frequency. It is based on the interaction of an external field with the electric dipole moment of the sample which is expressed by permittivity.

Impedance of a system is measure over a range of frequencies which reveals the frequency response of the system, including the dissipation properties and energy storage of the system.

Dielectric spectroscopy is used to measure the complex impedance, permittivity and conductivity spectra by varying the frequency and temperature of the sample material. Many key aspects of material properties can be derived from the frequency and temperature dependent measured spectra.

Fig 3.8 Dielectric spectrometer equipment used in the Dielectric characterization of La_2NiMnO_6

3.3.5 **Activation Energy:**

Activation Energy is the minimum energy required for a chemical reaction to occur. It can be understood as the potential barrier which must be reached for any reaction to proceed at the reasonable rate. The quantitative relation between the activation energy and the rate at which a reaction proceeds is given by the Arrhenius equation.

Arrhenius equation is given as:

$K=Ae^{-Ea/RT}$

Where A is the frequency factor, R is the universal gas constant, T is the temperature (in kelvin), and k is the reaction rate coefficient, E_a is the activation energy.

Even without knowing A, we can calculate the value of E_a from the variation in reaction rate coefficients as a function of temperature.

The readings were noted down with the 6517 A Electrometer / High Resistance Meter. Using these reading graph is been drawn with the help of origin software.

Fig 3.9 Equipment used for the Activation Energy measurement of La_2NiMnO_6

CHAPTER 4

Results and Discussion

4.1 X- ray Diffraction Characterization

An X-ray powder diffraction (XRD) pattern of the La_2NiMnO_6 synthesized by solid state method is shown in fig 4.1. XRD pattern indicates the proper phase formation of monoclinic structure, which is consistent with previous studies. This pattern indicates that Ni and Mn ions in LNMO tend to occupy different atomic position and form ordered phase.

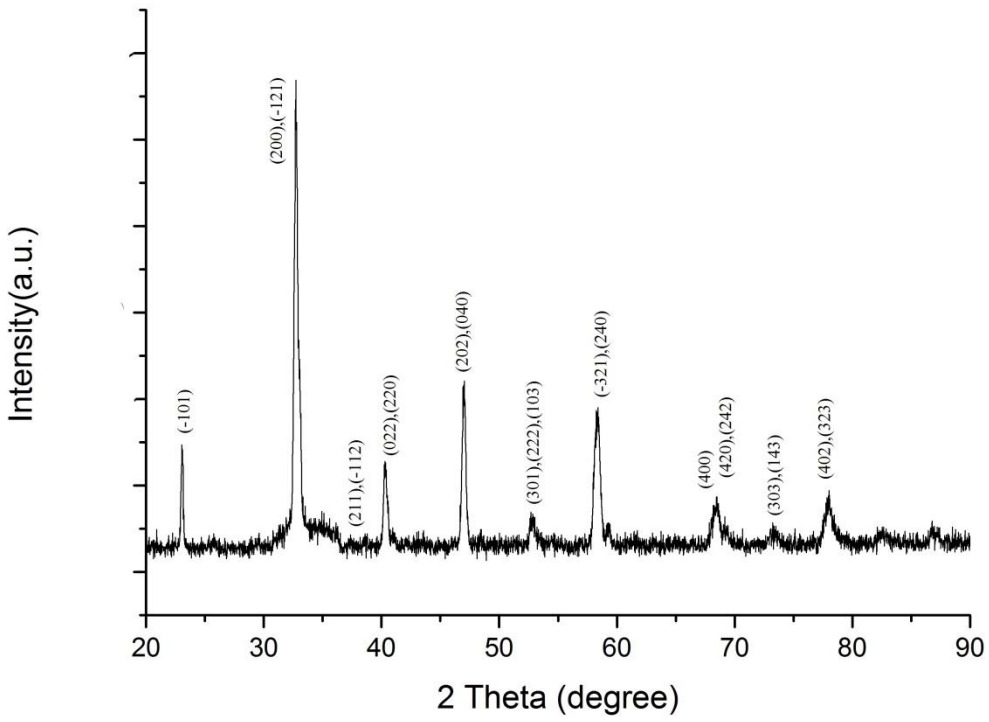

Fig 4.1 XRD pattern of the LNMO sample prepared by solid state method

4.2 Scanning Electron Microscope Characterization

Scanning Electron Microscope (SEM) images were taken at different magnification to analyze the surface morphology, particle size and shape of the prepared sample. Fig 4.2 represents the SEM images of the La_2NiMnO_6 synthesized by solid state method. The particle size of the prepared sample is about 1 μm as can be seen in fig below. It is observed that the particles are regular in shape and sample show agglomerate morphology.

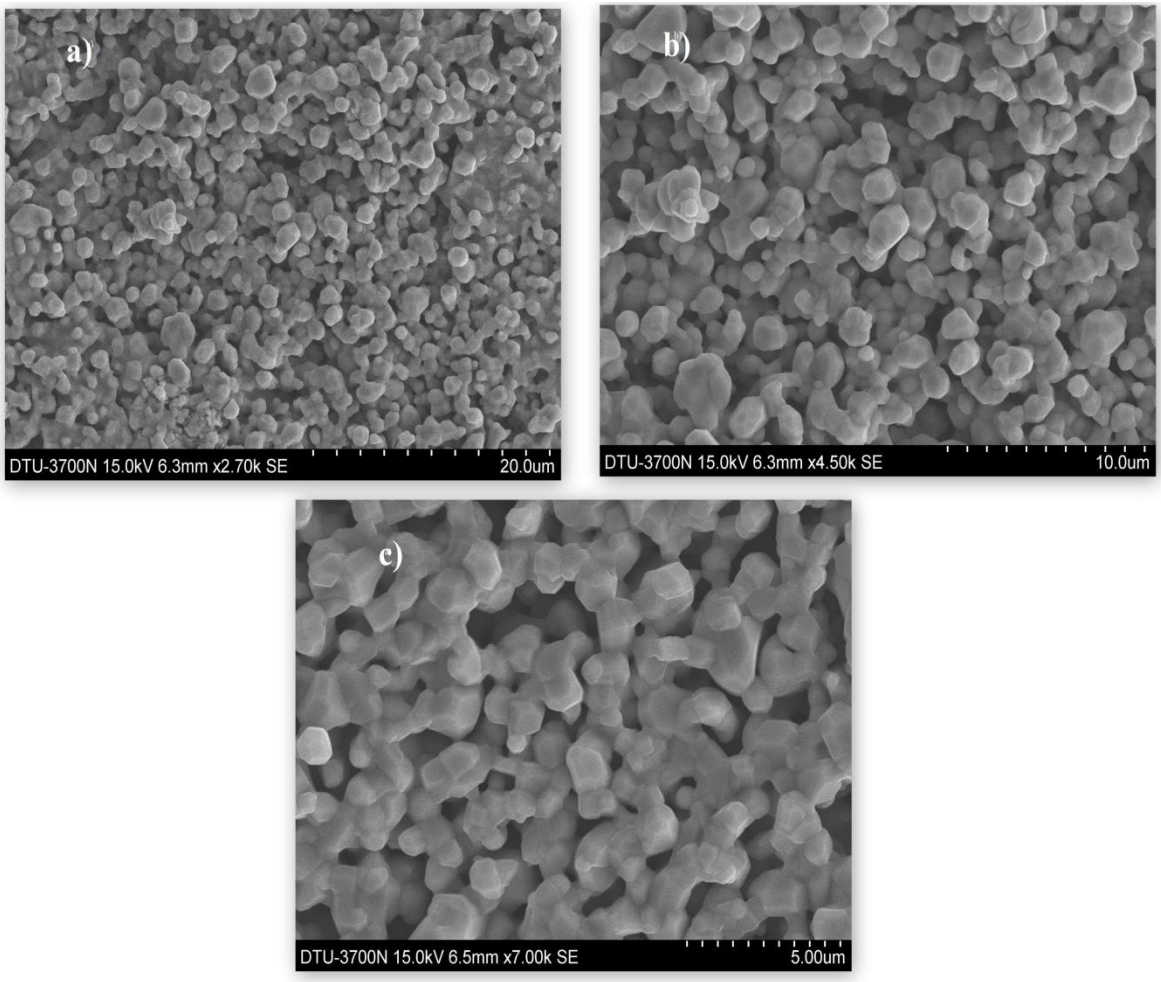

Fig 4.2 SEM images of the LNMO sample prepared by solid state method

a) At magnification of 20 μm b) At magnification of 10 μm c) At magnification of 5 μm

4.3 Energy Dispersive Spectroscopy (EDS)

EDS analysis of the La_2NiMnO_6 was carried out at accelerating voltage of 15 KV and take off angle 67.5°. The peaks of La, Ni and Mn are clearly visible in the EDS pattern of La_2NiMnO_6 synthesized by solid state method as shown in fig 4.3. Quantitative result obtained from the peaks of pattern is shown in table 4.1. It shows that the gold is present which had been coated on the sample to increase the conductivity of the sample. Some impurity of Aluminium is also seemed to be present in the prepared sample.

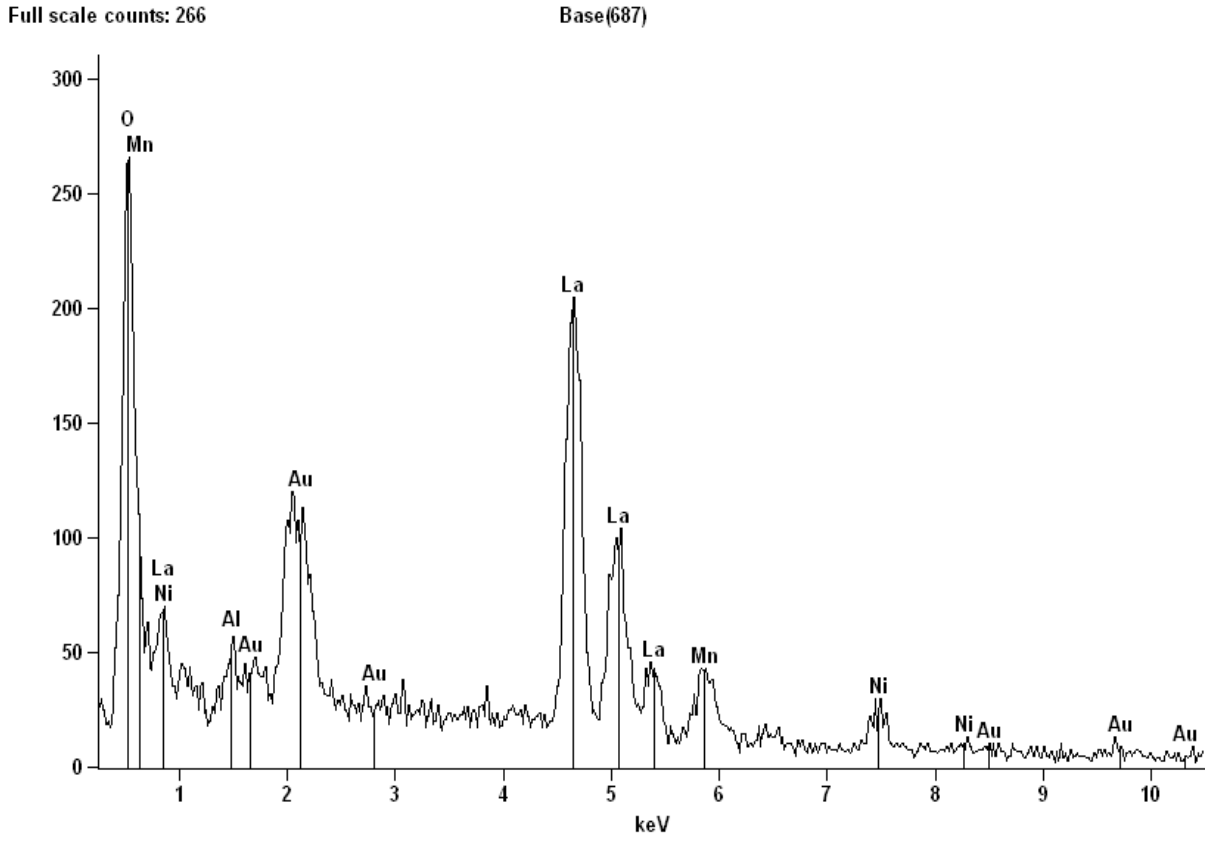

Fig 4.3 EDS pattern of La_2NiMnO_6 synthesized by solid state method

Table 4.1 Quantitative data of element in La_2NiMnO_6 observed by EDS

Element Line	*Net Counts*	*Int. Cps/nA*	*Weight %*	*Weight % Error*	*Atom %*	*Atom % Error*	*Formula*
O K	3808	---	19.04	+/- 0.52	61.48	+/- 1.68	O
Al K	158	---	0.68	+/- 0.15	1.29	+/- 0.28	Al
Mn K	493	---	7.49	+/- 0.82	7.04	+/- 0.77	Mn
Mn L	123	---	---	---	---	---	
Ni K	314	---	8.11	+/- 1.11	7.14	+/- 0.98	Ni
Ni L	74	---	---	---	---	---	
La L	5507	---	55.46	+/- 1.29	20.62	+/- 0.48	La
La M	913	---	---	---	---	---	
Au L	46	---	---	---	---	---	
Au M	1180	---	9.22	+/- 1.15	2.42	+/- 0.30	Au
Total			100.00		100.00		

4.4 Dielectric Measurement

The dielectric measurement of the sample La_2NiMnO_6 prepared using solid state method is shown in fig 4.4 and 4.5 which shows the temperature dependence of dielectric constant and dielectric loss from 133 k to 383 k at various applied frequencies ranging from 1 kHz to 1MHz. From fig 4.4 it is indicated that by increasing the temperature dielectric constant value of La_2NiMnO_6 sample increases almost linearly for most frequency at lower temperature but as temperature increases and reaches near room temperature it shows weak temperature dependence. Fig 4.5 shows the dielectric loss of the sample corresponding to the varying temperature. A dielectric loss peak occurs corresponding to the drop of the dielectric constant. The peak also shifts to lower temperatures with decreasing frequency, which indicates thermally activated relaxation process. The dielectric loss increases with the increase in temperature which is due to contribution of dc conductivity in La_2NiMnO_6.

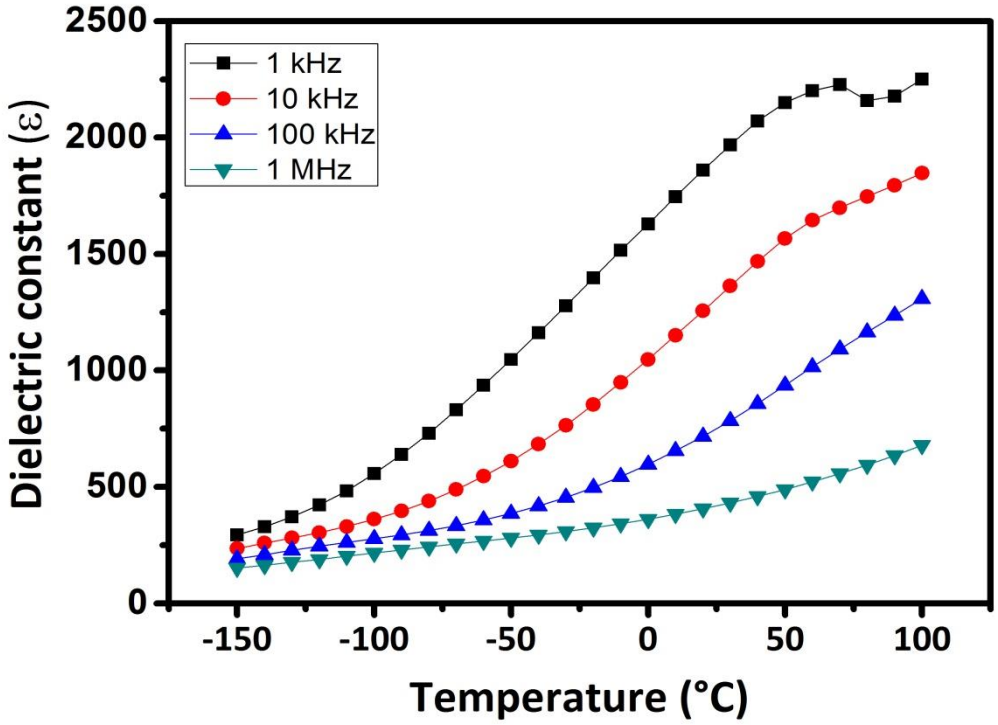

Fig 4.4 Temperature dependence of dielectric constant for La_2NiMnO_6 sample synthesized by solid state method at different frequencies.

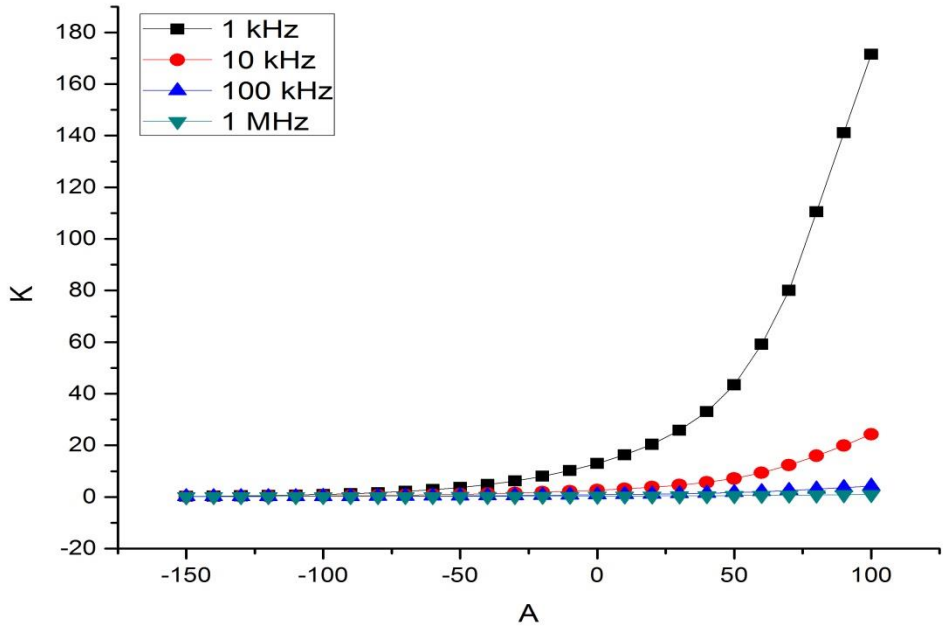

Fig 4.5 Temperature dependence of dielectric loss for La_2NiMnO_6 sample synthesized by solid state method at different frequencies.

4.5 Activation Energy

For activation energy calculation of the La_2NiMnO_6 reading of DC resistance were taken with variation in temperature. The temperature is varied from 20°C to 250°C. From the values of these reading and Arrhenius equation a graph is plotted between ln $(\sigma)_{DC}$ and the inverse of temperature. The graph for Activation Energy calculation of LNMO sample is shown in fig 4.6.

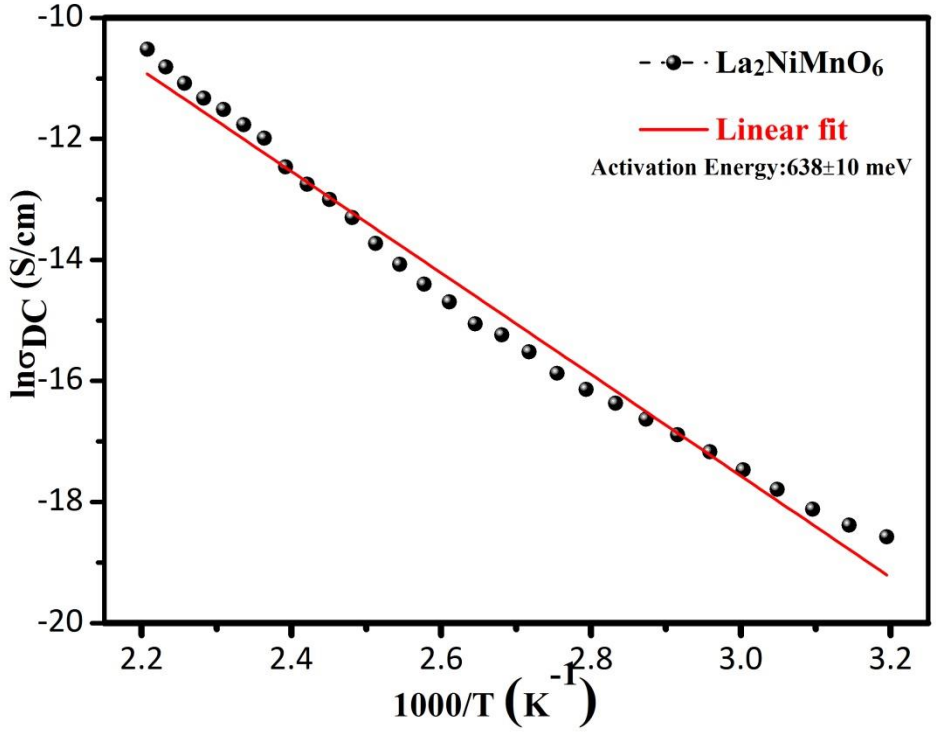

Fig 4.6 Graph for the Activation Energy calculation of La_2NiMnO_6 sample synthesized by solid state method.

With the help of the experimental values obtained from the analysis and Arrhenius Equation the Activation Energy for LNMO sample is calculated as

$E_a = 638 \pm 10$ meV

CHAPTER 5

Summary and Conclusions

The sample of LNMO ceramic has been prepared using solid state method by three stage thermal treatment for 20 hours at 1000°C, for 20 hours at 1200°C, for 20 hours at 1300°C. The XRD pattern indicates the proper phase formation of monoclinic structure which shows Ni and Mn ions form ordered phase. SEM result shows regular shape particles of LNMO about 1 μm in size. Dielectric properties measurement of the sample at various frequencies shows temperature dependency. Dielectric constant plateau peaks have been observed near room temperature and starts decreasing at higher temperature. The loss tangent of the LNMO increases corresponding to the drop in dielectric constant. Thus, the dielectric measurement of LNMO sample indicates the relaxor-like dielectric behavior. Activation energy of LNMO has been calculated to 638±10 meV, The obtained properties are suitable for fabricating magnetodielectric capacitors and spin filtering tunnel junctions.

References

1. https://en.wikipedia.org/wiki/Transition_metal
2. http://chem.libretexts.org/Core/Inorganic_Chemistry/Descriptive_Chemitry/Elements_Organized_by_Block/3_dBlock_Elements/1b_Properties_of_Transition_Metals/Electron_Configuration_of_Transition_Metals/Oxidation_States_of_Transition_Metals
3. https://en.wikipedia.org/wiki/Surface_properties_of_transition_metal_oxides
4. Tatsumi Ishihara. Perovskite Oxide for Solid Oxide Fuel Cells. Springer, Oxford, 2009
5. https://en.wikipedia.org/wiki/Perovskite_(structure)
6. Tadayuki Imai, Masahiro Sasaura, Koichiro Nakamura, Kazuo Fujiura. NTT Technical Review. Vol. 5 No. 9 Sep. 2007
7. M. T. Anderson, K. B. Greenwood, G. A. Taylor, K. R. Poeppelmeier. Prog. Solid State Chem., vol. 22, no. 3, pp. 197–233, 1993.
8. Sami Vasala, Maarit Karppinen. Progress in Solid State Chemistry 43 (2015) 1-36.
9. P. Kumar, S. Ghara, B. Rajeswara, D.V.S. Muthu, A. Sundaresan, A.K. Sood. Solid State Commun. 184 (2014) 47–51.
10. Nyrissa S. Rogado, Jun Li, Arthur W. Sleight, Mas A. Subramanian. Adv. Mater. 2005, 17, 2225-2227
11. Zhenzhu Cao, Xiaoting Liu , Weiyan He, Xuezheng Ruan, Yanfang Gao, Jinrong Liu. Physica B 477 (2015) 8–13
12. Yuqiao Guo, Lei Shi, Shiming Zhou, Jiyin Zhao, Wenjie Liu. Applied Physics Letters 102, 222401 (2013).
13. D. Choudhury, P. Mandal, R. Mathieu, A. Hazarika, S. Rajan, A. Sundaresan, U.V. Waghmare, R. Knut, O. Karis, P. Nordblad, D. D. Sarma. Physical Review Letters 108, 127201 (2012)
14. H. Z. Guo, J. Burgess, E. Ada, S. Street, A. Gupta. Physical Review B **77**, 174423 (2008)
15. Y.Q. Lin, X.M. Chen, X.Q. Liu. Solid State Communications 149 (2009) 784-787
16. Xueping Yuan, Qiuhang Li, Jianzhong Hu, Mingxiang Xu. Physica B 424 (2013) 73–78
17. Mazhar Ullah, Saleem Ayaz Khan, G. Murtaza, R. Khenata, Naeem Ullah, S. Bin Omran. Journal of Magnetism and Magnetic Materials 377 (2015) 197–203
18. Changnian Li, Bangxu Liu, Yanyan He, Chao Lv, Hua He, Yebin Xu. Journal of Alloys and Compounds 590 (2014) 541–545

19. https://en.wikipedia.org/wiki/X-ray_crystallography
20. Sulabha Kulkarni. Nanotechnology: Practices and principle. Springer, 2014
21. http://serc.carleton.edu/research_education/geochemsheets/techniques/SEM.html